Recognition of the 5′ Leader and the Acceptor Stem of a Pre-tRNA Substrate by the Ribozyme from *Bacillus subtilis* RNase P†

Andrew Loria and Tao Pan*

Department of Biochemistry & Molecular Biology, University of Chicago, Chicago, Illinois 60637

Received January 28, 1998; Revised Manuscript Received May 20, 1998

ABSTRACT: The catalysis by the ribozyme from bacterial RNase P involves specific interactions with the structure of the tRNA substrate. Recognition of the T stem−loop by this ribozyme occurs in a groove-like structure dictated by the tertiary folding of tRNA [Loria, A., and Pan, T. (1997) *Biochemistry 36*, 6317]. Effects of 2′-OH → 2′-H modifications within the acceptor stem and the 5′ leader on substrate binding and catalysis are determined using a $tRNA^{Phe}$ substrate that is significantly cleaved at more than one site. In all but one case, the 2′-deoxy substitution has little effect on binding for cleavage at the correct and incorrect sites. Substitution of the 2′-OH group at the correct site, however, decreases the cleavage chemistry by more than 3.4 kcal/mol for cleavage at both the correct and incorrect sites. Substitutions of the 2′-OH groups at the incorrect sites have no effect for cleavage at the incorrect and correct sites. Truncation of the 5′ leader results in differential effects on cleavage at different sites. These observations lead to a model in which cleavage at the correct and incorrect sites involves formation of different ribozyme−substrate complexes depending on binding of specific nucleotides in the 5′ leader. Binding of the T stem−loop of tRNA and the 2′-OH group at the correct cleavage site is common for all ES complexes. An A/U-rich 5′ leader significantly promotes formation of the ES complex and accelerates the cleavage chemistry over those of a C/G-rich 5′ leader, but only moderately enhances cleavage at the correct site over cleavage at the incorrect sites. Since cleavage at different sites requires formation of different ES complexes, cleavage site selection can occur at the level of the ES complex and at the chemical step.

Ribozyme catalysis requires specific recognition of the structure and/or sequence of the substrate and precise positioning of designated functional groups in the active site. The well-characterized *Tetrahymena* group I ribozyme recognizes its substrate initially through Watson−Crick base pairing in forming the P1 helix (*1*). The P1 helix is then precisely positioned into the active site through specific interactions between the catalytic core of the ribozyme with four 2′-OH groups and the exocyclic 2-amino group of a G·U wobble pair (*2*−*6*). How the P1 helix is positioned in the catalytic core determines the catalytic efficiency and the location of the cleavage site (*7*, *8*).

Substrate recognition and active site positioning for the ribozyme from bacterial RNase P involves RNA structures more complex than a single helix. Bacterial RNase P is composed of one 330−420-nucleotide RNA and a 13−15 kDa protein (*9*, *10*). RNase P is responsible for generating the mature 5′ end of all tRNAs in vivo through a specific endonucleolytic cleavage reaction. At high Mg^{2+} and monovalent ion concentrations, the RNA component alone (denoted P RNA) is nearly as active in vitro as the P RNA−P protein complex (*11*, *12*). P RNA primarily recognizes the T stem−loop and the acceptor stem−3′ CCA of a tRNA (*13*−*17*). The recognition of the T stem−loop occurs through tertiary interactions and contributes significantly to the affinity of the P RNA−tRNA complex (*18*). In contrast to the P1 helix in the group I ribozyme, the T stem−loop of a tRNA is more than 30 Å away from the reactive phosphate where catalysis is carried out. A large body of evidence suggests that the acceptor stem−3′ CCA region plays a pivotal role in the positioning of the reactive phosphate into the RNase P active site (*16*, *17*, *19*, *20*).

This paper describes the effects of site-specific modifications in the acceptor stem and in the 5′ leader on substrate binding and catalysis by the P RNA component of RNase P. The $tRNA^{Phe}$ substrate employed in this work is significantly cleaved at more than one site. Surprisingly, our results indicate that a single, specific 2′-OH group has an identically large effect on cleavage efficiency at all sites. This is in contrast to the group I ribozyme where different sets of 2′-OH groups are utilized for different cleavage sites. We provide evidence that cleavage at different sites involves interaction of different nucleotide residues in the 5′ leader. The 5′ leader nucleotide which is bound in the ES complex is a major determining factor in guiding the reactive phosphate into the active site.

MATERIALS AND METHODS

Modified tRNA Substrates. All tRNA substrates containing a single or double 2′-deoxynucleotide are prepared as described in ref *18*. All RNA oligonucleotides containing site-specific 2′-deoxy substitutions are custom synthesized using phosphoramidite chemistry by Dharmacon Research (Boulder, CO) with novel 2′ protecting groups (*21*). The

† This work was supported by grants from the NIH (GM52993) and the American Cancer Society (JFRA-543).

* Corresponding author. Telephone: (773) 702-4179. Fax: (773) 702-0439. E-mail: taopan@midway.uchicago.edu.

S0006-2960(98)00220-7 CCC: $15.00
Published on Web 06/20/1998

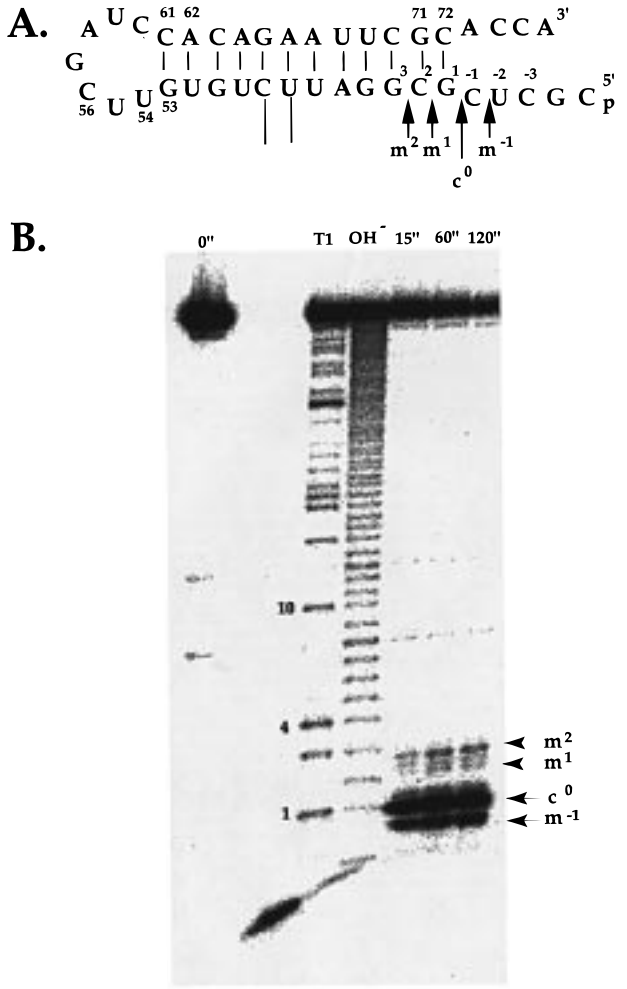

FIGURE 1: (A) Nomenclature of the nucleotides in the T stem−loop, the acceptor stem, and the 5′ leader region. The locations of the single 2′-OH → 2′-H substitutions are indicated by numbered nucleotides. (B) Cleavage at the correct and alternate sites using 5′ ^{32}P-labeled tRNA^{Phe} substrate. The T1 and OH$^-$ lanes indicate partial nuclease T1 digestion and alkaline hydrolysis of the same substrate. Cleavage at the correct site is designated as c^0, and cleavages at the alternate sites are designated as m^{-1}, m^1, and m^2. The 3′ ends of the c^0, m^{-1}, and m^2 5′ products using the 2′-ribosubstrate were confirmed by 5′ ^{32}pCp ligation followed by two-dimensional thin-layer chromatography (not shown). The smearing of the possible m^1 product shown here is attributed to comigration of the bromophenol blue dye marker. Due to the minute amount and ligation efficiency, the m^1 product was not analyzed by thin-layer chromatography.

substrate with the 3′ CCA deletion was prepared by ligating an RNA oligo containing nucleotides 49−73 of tRNA^{Phe} to the remainder of the substrate. The residue 1−72 mutants were made by ligating an oligoribonucleotide (−5 to 9 of the pre-tRNA^{Phe} substrate shown in Figure 1A) to RNA transcripts containing tRNA^{Phe} residues 10−76 with appropriate mutations.

Kinetics of the Cleavage Reaction. All kinetic measurements were performed under single-turnover conditions with a 10−10000-fold molar excess of P RNA over 5′ ^{32}P-labeled substrates. The final ribozyme concentrations range from 0.005 to 25 μM. The ribozyme and the substrates are renatured as described (*22*). The details of kinetic reactions are identical to those described in ref *18*. Unless noted otherwise, all reactions were carried out in 50 mM buffer (pH 6.1−8.1), 100 mM $MgCl_2$, and 0.6 M KCl at 37 °C.

The reaction rates for cleavage at the correct ($k_{obs}^{c^0}$) and incorrect ($k_{obs}^{m^2}$ and $k_{obs}^{m^{-1}}$) sites were determined using equations for parallel reactions (*23*). The amounts of individual reaction products [cpm(P)$_t$] and remaining substrate [cpm(S)$_t$] were quantitated. The sum of the reaction rates (k_{obs}) were obtained by fitting [fraction S remaining](t) = cpm(S)$_t$/[cpm(S)$_t$ + $\sum$cpm(P)$_t$] versus time (t) with a single-exponential function. The reaction rates for individual cleavage sites were calculated using the equations

$$k_{obs} = k_{obs}^{c^0} + k_{obs}^{m^2} + k_{obs}^{m^{-1}} \quad (1)$$

$$k_{obs}^{c^0} = [\text{cpm(P)}_t^{c^0}/\textstyle\sum \text{cpm(P)}_t]k_{obs} \quad (2)$$

$$k_{obs}^{m^2} = [\text{cpm(P)}_t^{m^2}/\textstyle\sum \text{cpm(P)}_t]k_{obs} \quad (3)$$

$$k_{obs}^{m^{-1}} = [\text{cpm(P)}_t^{m^{-1}}/\textstyle\sum \text{cpm(P)}_t]k_{obs} \quad (4)$$

An equilibrium binding constant (K^{c^0}) and the cleavage rate at saturating ribozyme concentrations (k^{c^0}) for cleavage at the c^0 site can be obtained using the equation

$$k_{obs}^{c^0} = k^{c^0}\left(\frac{[E]}{K^{c^0} + [E]}\right) \quad (5)$$

k^{c^0} and K^{c^0} are defined as the maximum cleavage rate and the ribozyme concentration at which the cleavage rate equals $k^{c^0}/2$ in single-turnover reactions, respectively. k^{c^0} and K^{c^0} are equivalent to k_{cat} and K_m in multiple-turnover reactions. They are used here to indicate that all kinetic parameters are obtained under single-turnover conditions.

For the miscleavage reactions, the formation of the ES$^{(c^0)}$ complex can be considered nonproductive binding. Hence, $K^{c^0} = K^{m^2} = K^{m^{-1}}$, and K^{c^0} is lower than the binding constant for the ES complex ($K_s = k_{-1}/k_1$; *23*). The k^{m^2} and $k^{m^{-1}}$ for the miscleavage sites are obtained by fitting $k_{obs}^{m^2}$ and $k_{obs}^{m^{-1}}$ versus [E] using the equations

$$k_{obs}^{m^2} = k^{m^2}\left(\frac{[E]}{K^{c^0} + [E]}\right) \quad (6)$$

$$k_{obs}^{m^{-1}} = k^{m^{-1}}\left(\frac{[E]}{K^{c^0} + [E]}\right) \quad (7)$$

Assuming the dissociation constants (k_{-1}) for the ES complex are much faster than k_2, we find that the actual K^{c^0} and k values are composed of the following terms:

$$1/K^{c^0} = 1/K_s^{c^0} + 1/K_s^{m^2} + 1/K_s^{m^{-1}} \quad (8)$$

$$k^{c^0} = k_2^{c^0}\left(1 + \frac{K_s^{c^0}}{K_s^{m^2}} + \frac{K_s^{c^0}}{K_s^{m^{-1}}}\right)^{-1} \quad (9)$$

$$k^{m^2} = k_2^{m^2}\left(1 + \frac{K_s^{m^2}}{K_s^{c^0}} + \frac{K_s^{m^2}}{K_s^{m^{-1}}}\right)^{-1} \quad (10)$$

$$k^{m^{-1}} = k_2^{m^{-1}}\left(1 + \frac{K_s^{m^{-1}}}{K_s^{c^0}} + \frac{K_s^{m^{-1}}}{K_s^{m^2}}\right)^{-1} \quad (11)$$

Table 1: Effects of Substrate Modification on K^{c^0} and k^{c^0} with Substrates Containing a 2′-Deoxynucleotide at the c^0 Site

substrate[a]	K^{c^0} (μM)	$\Delta\Delta G$ (K^{c^0})[b]	k^{c^0} (min^{-1})	$\Delta\Delta G$ (k^{c^0})[b]	$\Delta\Delta G$ (k^{c^0}/K^{c^0})[b]
(d−1)	0.14 ± 0.03	−	2.7 ± 0.2	−	−
d71	0.39 ± 0.08	0.6	2.0 ± 0.1	0.2	0.8
d72	0.27 ± 0.07	0.4	1.3 ± 0.1	0.4	0.8
d+1	0.28 ± 0.08	0.4	2.4 ± 0.2	0.1	0.5
d+2	0.22 ± 0.03	0.3	2.6 ± 0.1	0.0	0.3
d+3	0.31 ± 0.03	0.5	3.7 ± 0.1	−0.2	0.3
d−3	0.18 ± 0.05	0.2	2.5 ± 0.2	0.0	0.2
d−2	0.83 ± 0.13	1.1	2.3 ± 0.2	0.1	1.2
ΔCCA[c]	1.6 ± 0.3	1.5[c]	0.29 ± 0.02	0.8[c]	2.3
A1·U72	0.32 ± 0.04	0.5	0.43 ± 0.02	1.1	1.6
C1·G72	0.08 ± 0.01	−0.3	6.3 ± 0.2	−0.5	−0.8
U1·A72	0.22 ± 0.05	0.3	1.9 ± 0.2	0.2	0.5

[a] Conditions: 50 mM Tris-HCl (pH 8.1), 100 mM $MgCl_2$, and 0.6 M KCl at 37 °C unless noted otherwise. [b] $\Delta\Delta G$ in kilocalories per mole at 37 °C. [c] Conditions: 50 mM Tris-HCl (pH 7.8), 100 mM $MgCl_2$, and 0.6 M KCl at 37 °C.

where k_2 is the chemical step of the reaction at the respective cleavage sites.

RESULTS

Effects of single 2′-OH → 2′-H Substitutions in the Acceptor Stem and the 5′ Leader. Contributions of 2′-hydroxyl groups were first examined using a pre-$tRNA^{Phe}$ substrate containing two 2′-deoxy substitutions (Figure 1A), one of which was always at the cleavage site and slows the maximum cleavage rate of the single-turnover reaction by several hundred-fold (*18*, *24*). The cleavage reaction was carried out at slightly higher pH (∼8.1) than previous experiments (*18*) to fully explore the effects of single 2′-H substitutions on the cleavage rate. The nucleotides of interest in the acceptor stem include nucleotides 71 and 72 which were implicated to affect catalytic efficiency (*25*) and nucleotides 1−3 for their proximity to the cleavage site (referred to here as the c^0 site). The 2′-H substitutions at those five positions result in K^{c^0} increases of less than 3-fold (<0.6 kcal/mol), whereas k^{c^0} is affected by less than 2-fold (<0.5 kcal/mol, Table 1). The second-order constant, k^{c^0}/K^{c^0}, reflects the overall effect of the 2′-H substitution. For these five positions, the difference in k^{c^0}/K^{c^0} is less than 4-fold (<0.8 kcal/mol, Table 1). These effects are surprisingly small compared to those of the group I ribozyme reaction in which 2′-H substitution at equivalent positions 2, 3, and 72 generated effects on the order of 1.2−3.7 kcal/mol on substrate binding alone (*5*).

Three other changes in the vicinity of the cleavage site were also made to assess the nonhelical regions in the tRNA substrate (Table 1). Substitution of 2′-H at position −2 produced a 6-fold effect on K^{c^0} and almost no effect on k^{c^0}. Substitution of 2′-H at position −3 essentially has no effect. On the other hand, deletion of the 3′ CCA nucleotides significantly reduced K^{c^0} by 1.5 kcal/mol, k^{c^0} by 0.8 kcal/mol, and k^{c^0}/K^{c^0} by 2.3 kcal/mol. The 3′ CCA results are consistent with previous studies that established direct contacts between the CCA nucleotides and specific residues in the P RNA (*16*, *17*, *26*).

The above 2′-OH → 2′-H substitutions are carried out with substrates containing a 2′-H at the cleavage site. The effects of these substitutions are unexpectedly small compared to those in the group I ribozyme reaction. To ensure that such small effects are not due to the 2′-H at the cleavage site, four additional 2′-modified substrates containing a 2′-OH nucleotide at the cleavage site were analyzed kinetically (Table 2). Although the chemistry for a ribosubstrate at pH >7.0 is too fast for manual measurement, the strong pH dependence of k^{c^0} (*12*, *24*) allows convenient determination of K^{c^0} and k^{c^0} at lower pH. Effects of the 2′-OH → 2′-H substitution in the ribosubstrate background are identically small compared to those in the deoxy substrate background (Table 2).

Table 2: Effects of Substrate Modification on K^{c^0} and k^{c^0} with Substrates Containing a 2′-Ribonucleotide at the c^0 site

substrate[a]	k^{c^0} (μM)	$\Delta\Delta G$ (K^{c^0})[b]	k^{c^0} (min^{-1})	$\Delta\Delta G$ (k^{c^0})[b]	$\Delta\Delta G$ (k^{c^0}/K^{c^0})[b]
(r−1)	0.013 ± 0.004	−	1.8 ± 0.1	−	−
d+1	0.019 ± 0.001	0.2	1.5 ± 0.02	0.1	0.3
d+2	0.022 ± 0.004	0.3	2.3 ± 0.1	−0.2	0.1
d+3	0.022 ± 0.003	0.3	2.4 ± 0.1	−0.2	0.1
d−3	0.021 ± 0.002	0.3	2.8 ± 0.1	−0.3	0.0

[a] Conditions: 50 mM MES (pH 6.1), 100 mM $MgCl_2$, and 0.6 M KCl at 37 °C. [b] $\Delta\Delta G$ in kilocalories per mole at 37 °C.

Effects of 1·72 Base Pair Mutations. The 1·72 base pair in the acceptor stem is sterically accessible from both the major and minor groove sides and has been suggested to participate in the P RNA−tRNA interaction (*9*). Mutation of this base pair in our $tRNA^{Phe}$ substrate from G1·C72 to three other Watson−Crick base pairs produced different effects depending on the identity of the base pair (Table 1). The largest effect was observed in k^{c^0}/K^{c^0} (1.6 kcal/mol) with the A1·U72 mutant; otherwise, the effects are modest. Further analysis of the U1·A72 mutant suggests, however, that the effect on K^{c^0} can be larger at lower Mg^{2+} concentrations ($\Delta\Delta G$ = 1.1 kcal/mol at 40 mM $MgCl_2$, data not shown). Therefore, the G1·C72 base pair should be preferred under physiological conditions, i.e., low Mg^{2+} concentrations.

Miscleavage of the $tRNA^{Phe}$ Substrate. Cleavage of the phosphodiester bond at alternate sites can be visualized easily on high-resolution denaturing gels due to their different sizes (Figure 1B). For the yeast $tRNA^{Phe}$ substrate with five nucleotides in the 5′ leader, three major miscleavage sites are apparent. These miscleavage products are due to cleavage of phosphodiester bonds at positions −1, 1, and 2, respectively (Figure 1A). Miscleavage in P RNA catalysis has been observed on numerous occasions, including cleavage of the natural pre-$tRNA^{His}$ substrate (*27*−*31*). The precise location of miscleavage sites and their extents vary depending on the particular substrate used. To our knowledge, a mechanistic model accounting for these miscleavage reactions is still lacking. We have initiated a systematic investigation to uncover the dominant factors that influence these miscleavage reactions. In the subsequent description of this work, we refer to the cleavage at the correct site as the "c^0 site" and the cleavage between nucleotides C^2G^3 and $U^{-2}C^{-1}$ as the "m^2 site" and "m^{-1} site", respectively (Figure 1B). The cleavage between nucleotides G^1C^2 (m^1 site) is not further considered in this work due to the lack of sensitivity and resolution on polyacrylamide gels.

The pH dependence of k^{c^0}, k^{m^2}, and $k^{m^{-1}}$ can reveal whether comparable rate-limiting steps are still observed for the cleavage at these sites. k^{m^2} and $k^{m^{-1}}$ for the substrate with a

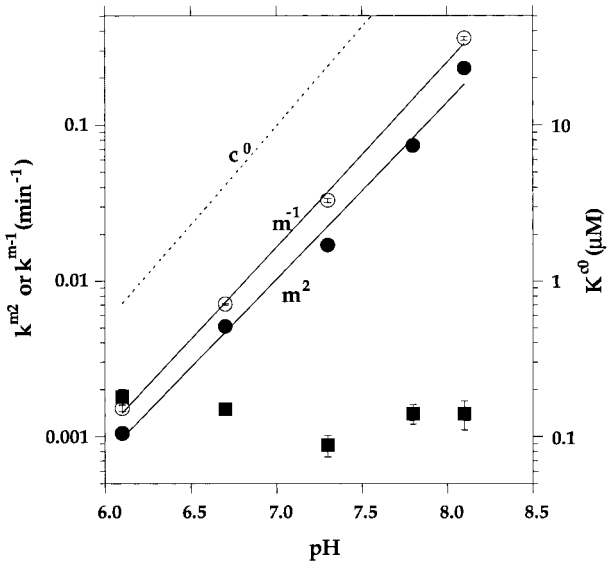

FIGURE 2: pH dependence of K^{c^0} (squares), k^{m^2} (filled circles), and $k^{m^{-1}}$ (open circles). All reactions were carried out with 50 mM buffer (pH 6.1−8.1), 100 mM $MgCl_2$, and 0.6 M KCl at 37 °C. The pH dependence of log(k^{m^2} or $k^{m^{-1}}$) has a slope of 1.1−1.2, corresponding to a factor of ∼200 from pH 6.1 to 8.1. The pH dependence of K^{c^0} is less than 2-fold from 6.1 to 8.1. The pH dependence of k^{c^0} is indicated as a dashed line (from ref *18*).

Table 3: Effects of T Stem−Loop Modification and P RNA Mutations on m^2 Cleavage

substrate[a]	K^{m^2} (μM)[b]	$\Delta\Delta G$ (kcal/mol)	k^{m^2} (min^{-1})[b]	$\Delta\Delta G$ (kcal/mol)
(d−1)	0.14 ± 0.02	−	0.074 ± 0.004	−
d54	1.4 ± 0.3	1.4	0.095 ± 0.005	−0.2 (0.5)[c]
d61	1.1 ± 0.4	1.3	0.079 ± 0.005	0.0 (0.0)
d62	2.1 ± 0.4	1.7	0.031 ± 0.001	0.5 (−0.1)
d53[d]	2.3 ± 0.7	1.7[d]	0.36 ± 0.02	−0.3 (1.0)[d]
d56	0.77 ± 0.17	1.0	0.059 ± 0.002	−0.1 (0.3)
A19·U56	1.0 ± 0.4	1.2	0.034 ± 0.002	0.5 (−0.5)
C19·G56	1.9 ± 0.1	1.6	0.024 ± 0.001	0.7 (−0.4)
d57	0.16 ± 0.06	0.1	0.035 ± 0.002	0.5 (0.2)
G130·d−1	2.8 ± 0.5	1.8	0.021 ± 0.001	0.8 (0.1)
G230·d−1	24 ± 3	3.2	0.0071 ± 0.0002	1.4 (0.0)

[a] All substrates contain a 2′-deoxynucleotide (d−1) at the c^0 site. [b] Conditions: 50 mM Tris-HCl (pH 7.8), 100 mM $MgCl_2$, and 0.6 M KCl at 37 °C. [c] $\Delta\Delta G^{c^0} - \Delta\Delta G^{m^2}$ in parentheses. Negative indicates improved c^0 over m^2; positive indicates improved m^2 over c^0. [d] Conditions: 50 mM Tris-HCl (pH 8.1), 100 mM $MgCl_2$, and 0.6 M KCl at 37 °C.

2′-H nucleotide at the c^0 site have a nearly log linear dependence on pH, and the rates are 8−12-fold slower than cleavage at the c^0 site over the same pH range (Figure 2). A decrease in [Mg^{2+}] from 100 to 40 mM or [K^+] from 0.6 to 0 M also resulted in a k^{m^2} decreased to the same extent as k^{c^0} (data not shown and ref *18*). These results suggest that for this substrate, cleavage at the correct and incorrect sites is governed by similar rate-limiting steps.

The effects of T stem−loop modifications and P RNA mutants on cleavage at the m^2 site (Table 3) are essentially identical to those at the c^0 site (*18*). Each 2′-OH → 2′-H modification at positions directly involved in P RNA−tRNA contact produced a loss of 1.0−1.7 kcal/mol for K^{m^2} (tRNA residues 54, 61, 62, 56, and 53). Also similar to c^0 cleavage, the changes in k^{m^2} are small for modified substrates compared to those for the unmodified substrate. Considering the $\Delta\Delta G$ of k^{c^0} versus k^{m^2}, the only significant difference ($\Delta\Delta G^{c^0} - \Delta\Delta G^{m^2} > 0.5$ kcal/mol) is for 2′-OH → 2′-H substitution at position 53. P RNA mutants known to affect direct T stem−loop interactions (P RNA residues A130 → G and A230 → G; *18*) have identical effects on m^2 cleavage. These results indicate that cleavage at the m^2 site depends on specific recognition of the T stem−loop very much like cleavage at the c^0 site.

Table 4: Effects of Substrate Modification on m^2 and m^{-1} Cleavage

substrate[a]	k^{m^2} (min^{-1})	$\Delta\Delta G$ (kcal/mol)	$k^{m^{-1}}$ (min^{-1})	$\Delta\Delta G$ (kcal/mol)
(d−1)	0.23 ± 0.01	− (−1.5)	0.36 ± 0.01	− (−1.2)
d71	0.15 ± 0.01	0.3 (−0.1)[b]	ND[c]	
d72	0.063 ± 0.004	0.8 (−0.4)	ND[c]	
d+1	0.19 ± 0.01	0.1 (0.0)	0.39 ± 0.03	0.0 (0.1)
d+2	0.18 ± 0.01	0.1 (−0.1)	0.77 ± 0.03	−0.5 (0.5)
d+3	0.13 ± 0.01	0.4 (−0.6)	0.72 ± 0.01	−0.4 (0.2)
d−3	0.08 ± 0.01	0.6 (−0.6)	0.50 ± 0.03	−0.2 (0.2)
d−2	0.11 ± 0.01	0.5 (−0.4)	0.43 ± 0.02	−0.1 (0.2)
ΔCCA[d]	0.048 ± 0.003	0.3 (0.5)[d]	ND[c]	
A1·U72	0.29 ± 0.01	−0.1 (1.2)	0.20 ± 0.02	0.4 (0.7)
C1·G72	0.42 ± 0.01	−0.4 (−0.1)	1.07 ± 0.09	−0.7 (0.2)
U1·A72	0.38 ± 0.02	−0.3 (0.5)	0.40 ± 0.01	−0.1 (0.3)
(r−1)	0.22 ± 0.01	− (−1.3)	0.71 ± 0.02	− (−0.6)
d+1	0.11 ± 0.01	0.4 (−0.3)	0.22 ± 0.01	0.7 (−0.6)
d+2	0.25 ± 0.02	−0.1 (−0.1)	0.56 ± 0.02	0.2 (−0.4)
d+3	0.25 ± 0.01	−0.1 (−0.1)	0.64 ± 0.02	0.1 (−0.3)
d−3	0.19 ± 0.01	0.1 (−0.4)	0.76 ± 0.02	0.0 (−0.3)

[a] Conditions: 50 mM Tris-HCl (pH 8.1) [2′-H (c^0) substrates, rows 1−12] or 50 mM MES (pH 6.1) [2′-OH (c^0) substrates, rows 13−17], 100 mM $MgCl_2$, and 0.6 M KCl at 37 °C. [b] $\Delta\Delta G^{c^0} - \Delta\Delta G^{m^2/m^{-1}}$ in parentheses. Negative indicates improved c^0 over m^2/m^{-1}; positive indicates improved m^2/m^{-1} over c^0. [c] m^{-1} cleavage not determined due to poor resolution. [d] Conditions: 50 mM Tris-HCl (pH 7.8), 100 mM $MgCl_2$, and 0.6 M KCl at 37 °C.

We next examined the effects of single atom modifications in the acceptor stem and the 5′ leader on k^{m^2} and $k^{m^{-1}}$ (Table 4). With the substrates containing a 2′-H at the c^0 site, the effect of 2′-H substitution at all other positions is modest (<0.8 and <0.7 kcal/mol for m^2 and m^{-1} cleavage, respectively). Substitution of a single 2′-OH → 2′-H with substrates containing a 2′-OH at the c^0 site also produced only modest effects (<0.4 and <0.7 kcal/mol for m^2 and m^{-1} cleavage, respectively). For both 2′-deoxy (c^0) and 2′-ribo (c^0) substrates, the surprising result is that the 2′-OH → 2′-H modification at the m^2 and m^{-1} sites (d+2 and d−2, double underlined in Table 4) has no effect (<0.1 kcal/mol) for their respective cleavage sites. This is in contrast to the 2′-OH → 2′-H modification at the c^0 site that decreased the k^{c^0} by ∼240-fold (3.4 kcal/mol). In fact, elimination of the 2′-OH at the same position (c^0 site) simultaneously decreased k^{m^2} and $k^{m^{-1}}$ by ∼210 and ∼470-fold (3.3 and 3.8 kcal/mol), respectively. It appears that the 2′-OH at the c^0 site affects the cleavage rate at all observable sites to the same extent.

Deletion of the 3′ CCA and mutation of the 1·72 base pair affect cleavage at each site differently (Table 4). The 3′ CCA deletion decreases k^{m^2}, but to a lesser extent than that for k^{c^0}. Other Watson−Crick base pairs at the 1·72 position show modest effects; in particular, the A1·U72 mutant does not affect k^{m^2}, as opposed to k^{c^0}. These results show that unlike 2′-OH (c^0), the effect of base changes in this region is unique for each cleavage site.

Effects of the Length and Sequence of the 5′ Leader. In addition to the 2′-OH at the c^0 site, the length and the

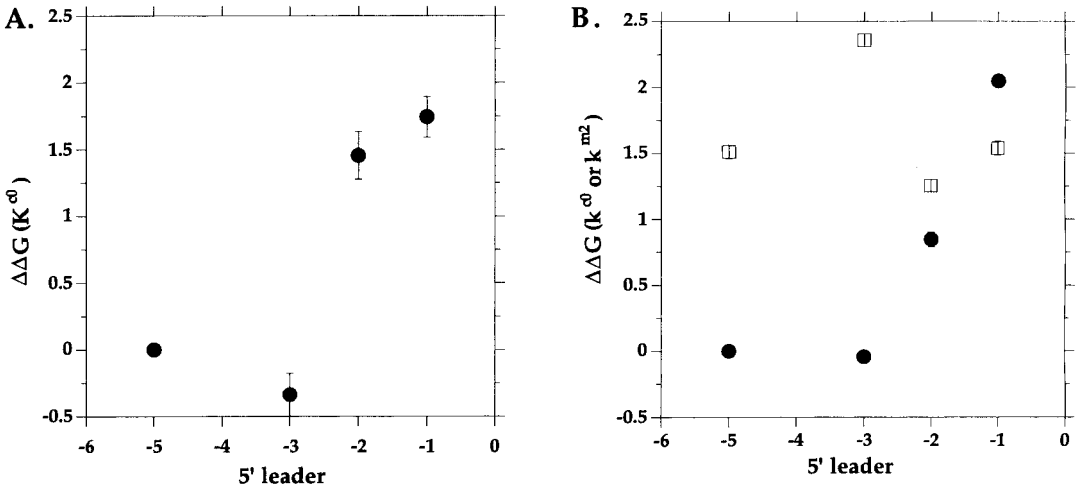

FIGURE 3: Effects of 5′ leader truncations on (A) K^{c^0} and (B) k^{c^0} (●) and k^{m^2} (□). All reactions were carried out using substrates with a 2′-H at the c^0 site with 50 mM Tris-HCl (pH 8.1), 100 mM $MgCl_2$, and 0.6 M KCl at 37 °C. The 5′ leader sequences for the truncated substrates are 5′CGCUdC (−5), 5′CUdC (−3), 5′UdC (−2), and 5′dC (−1). The $\Delta\Delta G$ values are relative to the c^0 cleavage of the −5 substrate.

sequence of the 5′ leader may also contribute to cleavage at the c^0 and other sites. The *Escherichia coli* P RNA (M1 RNA) can cleave tRNA substrates with a single nucleotide in the 5′ leader with a rate comparable (*24*) to that of our *Bacillus subtilis* P RNA−$tRNA^{Phe}$ pair at pH 6. However, two to three nucleotides were needed to protect specific residues in P RNA from chemical modification (*17*) or to induce P RNA−substrate photo-crosslinks (*32*). Deletion of the −5 and −4 nucleotides of our $tRNA^{Phe}$ substrate has essentially no effect (Figure 3). Further truncation produces strong effects on both k^{c^0} (up to 2.0 kcal/mol) and K^{c^0} (up to 1.7 kcal/mol). However, the substrates with either five or one nucleotide 5′ leader have identical k^{m^2} values (Figure 3). Using the $tRNA^{Phe}$ product (equivalent to deletion of the −1 nucleotide), m^2 cleavage can no longer be detected, even after overnight incubation. In addition, the m^{-1} cleavage was undetectable for the substrate with only three nucleotides in the 5′ leader. These observations indicate that the interaction concerning the third nucleotide 5′ to the respective cleavage site determines to a large extent which phosphodiester bond is hydrolyzed.

Although the 5′ leader sequences of natural tRNA precursors are not conserved, they are often A/U-rich (*33*−*35*). All substrates described above contain a C/G-rich 5′ leader (5′ CGCUC). To quantitatively analyze the potential effects of an A/U-rich leader sequence, two substrates containing 100% A/U (5′ AAUAU) in the 5′ leader are compared to the substrates with the 5′ C/G-rich sequence (Table 5). Cleavage at the m^{-1} site was not quantitated due to limitations in gel resolution. The A/U-rich leader significantly improves k^{c^0} and k^{m^2} compared to those of the C/G-rich 5′ leader. When k^{c^0}/K^{c^0} and k^{m^2}/K^{m^2} are compared, the A/U-rich sequence moderately increases the cleavage site selection at the c^0 site compared to that at the m^2 site by 0.5−0.9 kcal/mol.

Table 5: Effects of the 5′ Leader Sequence on Cleavage at the c^0 and m^2 Sites

substrate	K^{c^0} (μM)	$\Delta\Delta G$ (kcal/mol)[c]	k^{c^0} or k^{m^2} (min^{-1})	$\Delta\Delta G$ (kcal/mol)[c]
Substrates with 2′-H at the c^0 site[a]				
5′ CGCUdC	0.088 ± 0.014	−	c^0, 0.19 ± 0.01	−
		−	m^2, 0.017 ± 0.001	−
5′ AAUAdU	0.022 ± 0.007	−0.9	c^0, 3.7 ± 0.2	−1.8
		−	m^2, 0.068 ± 0.003	−0.9
Substrates with 2′-OH at the c^0 site[b]				
5′ CGCUC	0.013 ± 0.004	−	c^0, 1.8 ± 0.1	−
		−	m^2, 0.22 ± 0.01	−
5′ AAUAU	0.022 ± 0.004	0.3	c^0, 6.8 ± 0.3	−0.8
			m^2, 0.38 ± 0.02	−0.3

[a] Conditions: 50 mM HEPES (pH 7.3), 100 mM $MgCl_2$, and 0.6 M KCl at 37 °C. [b] Conditions: 50 mM MES (pH 6.1), 100 mM $MgCl_2$, and 0.6 M KCl at 37 °C. [c] $-RT \ln[K^{c^0}(CG)/K^{c^0}(AU)]$ or $-RT \ln[k^{c^0}$ or $k^{m^2}(AU)/k^{c^0}$ or $k^{m^2}(CG)]$.

DISCUSSION

Miscleavage of the Pre-$tRNA^{Phe}$ Substrate. The appearance of substantial amounts of miscleavage products in our $tRNA^{Phe}$ substrate invokes the question of cleavage site selection for other tRNA substrates. The tRNA substrates in many published works have long, A/U-rich 5′ leaders, and miscleavages as extensive as that in our $tRNA^{Phe}$ substrate are seldom seen. As observed for our A/U-rich substrates, the natural A/U-rich 5′ leaders may allow preferential interaction between the ribozyme and the substrate to selectively promote c^0 cleavage. In addition, reliable quantitation for any miscleavage product in the background of c^0 cleavage is ≤1%, only 2−5-fold less miscleavage than in our yeast $tRNA^{Phe}$ substrate with an A/U-rich 5′ leader [∼2 and ∼5% for the 2′-H (c^0) and 2′-OH (c^0) substrates, respectively]. It is conceivable that many tRNA substrates may miscleave, but the miscleavage has not yet been deliberately examined.

What then determines that our $tRNA^{Phe}$ substrate is miscleaved to such a high extent? When the holoenzyme was used under physiological conditions with our substrates with 5′ leaders containing five nucleotides, no significant change in the cleavage pattern was observed (A. Loria and T. Pan, manuscript in preparation). The holoenzyme result does not preclude the possibility that long, A/U-rich 5′ leaders may interact specifically with the holoenzyme (*36*) to contribute selectively to c^0 cleavage. Although our $tRNA^{Phe}$ substrate and P RNA are from different sources, the catalytic efficiency (k^{c^0}/K^{c^0}) of the yeast $tRNA^{Phe}$−*B. subtilis* P RNA combination is close to those of the *B. subtilis* $tRNA^{Asp}$−*B. subtilis* P RNA combination. A similar miscleavage pattern

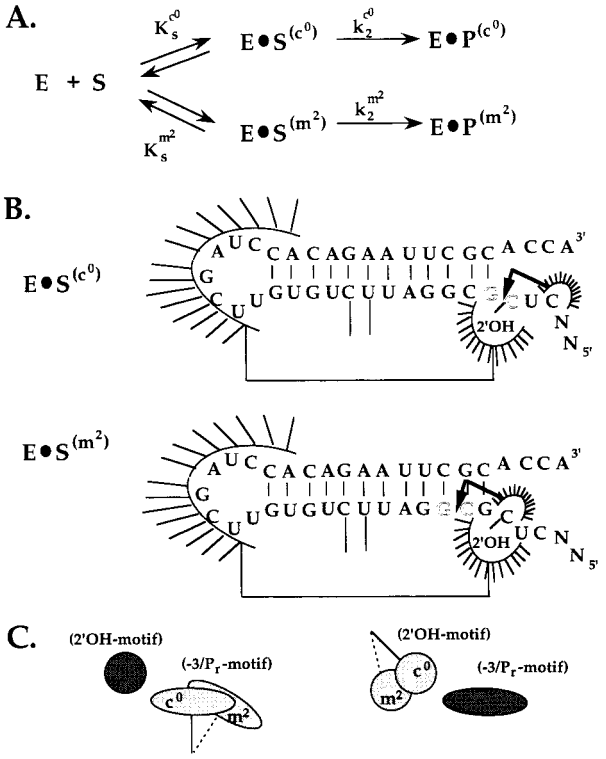

FIGURE 4: (A) Multiple ES complex model in the kinetic scheme of the P RNA reaction. The binding and the chemical step are indicated by the equilibrium constant K_s (*23*) and k_2, respectively. (B) The proposed molecular composition of the ES(c^0) and ES-(m^2) complexes incorporating the data from this work. The binding sites in the ribozyme are shown as hatched half-ovals. The bound T stem−loop directs binding of the 2′-OH(c^0) as shown by a thin line. Binding of the third nucleotide 5′ to the cleavage site directs which phosphodiester (between the highlighted nucleotides) is positioned into the active site as shown by a thick line and an arrow to indicate cleavage. (C) Two models for the binding motifs in the catalytic domain of P RNA and their relative juxtaposition in the ES complex. The flexible motif in the unbound form is indicated by a connecting line and is gray. The inflexible motif in the unbound form is black. (Left) The $-3/P_r$ motif (oval) is flexible; (right) the 2′-OH motif (circle) is flexible.

also occurs for the yeast $tRNA^{Phe}$−*E. coli* P RNA pair (A. Loria and T. Pan, data not shown). Therefore, the relatively high efficiency of miscleavage observed in our substrate appears to be correlated with the identity of the particular $tRNA^{Phe}$ sequence. This strong tRNA dependence is consistent with the reports that the predominant factor for cleavage site selection of the naturally miscleaving $tRNA^{His}$ is the acceptor stem sequence (*28*, *37*).

Substrate Components in Binding and Catalysis. A simple model with formation of different ES complexes for cleavage at different sites can be proposed to explain all experimental data presented here (Figure 4A). For simplicity, only c^0 and m^2 cleavages are discussed below, although the conclusion applies equally well to m^{-1} cleavage. The molecular composition of the distinct ES complexes can be deduced from several key observations in this work (Figure 4B).

(1) The T Stem−Loop of the tRNA. Cleavage at the m^2 site depends on the T stem−loop (TSL) to a similar extent as cleavage at the c^0 site, suggesting that binding of TSL is nearly the same for all ES complexes. The TSL region directly interacts with P RNA through at least five 2′-OH groups and the 4-amino group of C56 (*18*). These six interactions alone contribute a net total of 8.3 kcal/mol in binding. For k^{c^0} and k^{m^2}, the effect is 1.6 and 0.4 kcal/mol, respectively (Table 3). The difference in k^{c^0} and k^{m^2} is mainly attributed to a single interaction involving the 2′-OH of residue 53. Otherwise, the TSL−P RNA interaction provides a similar affinity for binding and catalysis. Recognition of the T stem−loop confers specificity to the P RNA for the tRNA substrates.

(2) The 2′-Hydroxyl at the c^0 Site. The 2′-OH → 2′-H substitution at the c^0 site changes the reaction kinetics for all cleavages to a similar extent, suggesting that the ribozyme interaction with this 2′-OH group is universal for all ES complexes. Substitution of 2′-OH with 2′-H at this position increases K^{c^0} by 1.4 kcal/mol and decreases the k^{c^0}, k^{m^2}, and $k^{m^{-1}}$ by more than 3.3 kcal/mol. The selection of this 2′-OH for all cleavage sites may be directed by T stem−loop binding (Figure 4B). Several functions for the 2′-OH group at the c^0 site have been proposed previously. Smith and Pace (*24*) suggested that it may be involved in binding and positioning of the Mg^{2+} ions for the chemical step. Alternatively, it may be involved in lowering the pK_a of the neighboring 3′-oxygen leaving group, analogous to the mechanism proposed for the group I ribozyme reaction (*4*). Both mechanisms would predict that 2′-OH groups at the c^0, m^{-1}, or m^2 site should significantly affect cleavage efficiency at the c^0, m^{-1}, or m^2 site, respectively. Such results are not observed in this work. The 2′-OH (c^0) can still be involved in binding of a Mg^{2+} ion necessary for maximal efficiency in chemistry. A Mg^{2+} of this kind may be distinct from the two other Mg^{2+} ions proposed to act as the base and the electrophile in the transition state (*38*).

(3) Other 2′-OH Groups and the Acceptor Stem of tRNA. 2′-OH at m^2 and m^{-1} sites does not contribute to cleavage at the respective sites. Substitution of a single 2′-OH with 2′-H in the acceptor stem of tRNA results in a small, uniform decrease in the equilibrium binding constant and has little effect on the cleavage rate, suggesting that the acceptor stem remains helical in the ground state. Whether the acceptor stem has to open in the transition state for c^0 cleavage is not clear. For m^2 cleavage, however, the acceptor stem helix has to open to allow binding of the phosphate at the m^2 site. Our data show no discernible differences for all m^2 cleavage steps using the 2′-H-substituted substrates, suggesting that helix melting for m^2 cleavage is not a rate-limiting step. In contrast to the role of the P1 helix in the group I ribozyme (*2*, *4*, *6*), no specific 2′-OH group in the acceptor stem appears to be involved in P RNA−tRNA interaction. Either potential acceptor stem−P RNA interaction is superfluous, or such interactions may decrease the dissociation rate of the P RNA−tRNA product and hinder the turnover of the RNase P reaction in vivo.

(4) The Third Nucleotide 5′ to the Respective Cleavage Site. Binding of this and, to some extent, the second nucleotide 5′ to the cleavage site directs binding of the reactive phosphodiester located two nucleotides away. The −3 and −2 nucleotides relative to the c^0 site are implicated in our truncation experiment to contribute 1.5−2.0 kcal/mol to binding and cleavage chemistry. Interaction of the −3 nucleotide with P RNA does not involve its 2′-OH; interaction of the −2 nucleotide does include its 2′-OH group. There is strong physical evidence for the direct −3 nucleotide−P RNA interaction as shown by chemical modification protection (*17*) and UV cross-linking (*32*). The −3 nucleotide

binding site in the P RNA has been mapped to the conserved J18/2 region (*17*). The effect of the −3 nucleotide positioning the reactive phosphate may be accomplished with a possible ruler mechanism. In this scenario, the binding site in the J18/2 region is 7−14 Å from the active site where chemistry at the reactive phosphate occurs. Two nucleotides are needed to bridge this distance.

(5) Other Substrate Components. In our model, binding of the reactive phosphodiester (P_r) is directed by the initial binding of the third nucleotide 5′ to it. Both the bridging and nonbridging oxygens can be involved in P_r binding. Hartmann and co-workers (*39*) have shown that *pro-*R_p and *pro-*S_p oxygens at the c^0 phosphate are involved in P RNA catalysis. Using phosphorothioate substitutions, the effect on k^{c^0} with a 2′-OH substrate for the *E. coli* P RNA is on the order of 4.7 and >6.4 kcal/mol for the *pro-*R_p and *pro-*S_p oxygens, respectively. Interestingly, miscleavage at the m^{-1} site is more severely affected for the *pro-*R_p than for the *pro-*S_p phosphorothioates. This observation may indicate that *pro-*R_p oxygen at the c^0 site plays a role similar to that of the 2′-OH at c^0 site (for cleavage at all sites), whereas the *pro-*S_p oxygen at this site may be exclusively involved in the chemical step (cleavage at the respective site). If this is the case, the *pro-*R_p O → S substitution at the c^0 site should affect all cleavage sites equally, whereas the *pro-*S_p O → S substitution should only affect the reaction at respective cleavage sites where the sulfur atom is located.

The 3′ CCA of the tRNA has been shown to interact directly with P RNA (*16*, *17*) and influence the cleavage efficiency at different sites (*29*−*31*). For our substrates, the main effect of the 3′ CCA is on K^{c^0} (1.5 kcal/mol). Interestingly, the 3′ CCA has a stronger effect on k^{c^0} than on k^{m^2}, even though deletion of 3′ CCA results in rate decreases for both sites. The net effect of this difference is increased miscleavage over the correct cleavage for the ΔCCA substrate. Such a 3′ CCA effect may also explain the preference switch of m^1 over m^2 cleavage using a substrate with a 5′ GGCUC leader rather than a 5′ CGCUC leader (data not shown). The $G^{-5}G^{-4}$ nucleotides can potentially interact with the 3′ CCA, making binding of the −1 nucleotide less likely to result in formation of smaller amounts of the ES complex committed for m^2 cleavage. Our results are consistent with observations by Kirsebom and co-workers (*16*, *30*), who have shown that modulating the 3′ CCA−P RNA interactions can produce strong differential effects on the correct and miscleavage sites for a variety of tRNA substrates.

Formation of the ES complex is strongly assisted by an A/U-rich compared to a C/G-rich 5′ leader sequence (Table 5). This observation is consistent with the natural pre-tRNA sequences from bacteria which are generally A/U-rich. Several explanations are possible for this A/U effect. (1) It has lesser potential to form secondary structures, making all nucleotides more available for P RNA binding. (2) The A/U sequence directly biases binding of the −3 nucleotide. (3) It does not form stable structures with the 3′ CCA to allow more efficient utilization of 3′ CCA. It remains to be seen which of the three effects dominates for the observed A/U-rich effect.

Potential Mechanisms for Cleavage Site Selection. Discrimination of cleavage sites (or proofreading) can occur at the levels of the ES complex (K_s) and the chemical step (k_2). The steric accessibility and affinity of the 5′ third nucleotide with respect to the respective cleavage site may determine the relative amount of ES complex formation. Our model proposes two distinct motifs in the ribozyme (designated the 2′-OH motif and the $-3/P_r$ motif in Figure 4C) that interact with residues around the cleavage site in the substrate. The interaction with the 2′-OH (c^0) significantly increases the cleavage efficiency but makes no distinction for cleavage site selection. The interaction with the third (and the second) nucleotide 5′ to the cleavage site determines the site of cleavage. In such a model, one of the two motifs is thought to be flexible prior to substrate binding. This may be accomplished structurally by linking one of the two motifs through a flexibly tethered loop (solid and dashed lines in Figure 4C). The flexibility of the $-3/P_r$ motif implies scanning the substrate within a confined range to bind the −3 nucleotide which leads to subsequent positioning of the reactive phosphate (Figure 4C, left). Alternatively, the flexibility of the 2′-OH motif implies scanning the substrate to bind the 2′-OH (c^0), regardless of which residues are bound in the $-3/P_r$ motif (Figure 4C, right). Binding of the 2′-OH (c^0) may increase the fraction of a putative ES complex along the reaction pathway prior to the chemical step of the reaction (k_2). Attempts to physically detect a second obligatory ES complex are being actively pursued in our laboratory.

Once the 2′-OH (c^0) and the −3 nucleotide−reactive phosphate are bound, the steric juxtaposition between these two motifs in the bound form of the ribozyme may influence the stability of the transition state. When the c^0 and m^2 complexes are compared, the 2′-OH motif is skewed relative to the $-3/P_r$ motif. The spatial relationship of these two motifs in the ES complex may be optimal for chemistry in the c^0 complex.

ACKNOWLEDGMENT

We thank Drs. Joseph Piccirilli, Tobin Sosnick, and Carl Correll for their stimulating discussions and comments on the manuscript. We also thank both reviewers for their comments, and in particular, we greatly appreciate the insightful comments of one reviewer on the reaction kinetics.

REFERENCES

1. Cech, T. R. (1993) in *The RNA World* (Gesteland, R., and Atkins, J., Eds.) pp 239−269, Cold Spring Harbor Laboratory Press, Plainview, NY.
2. Pyle, A. M., and Cech, T. R. (1991) *Nature 350*, 628−631.
3. Bevilacqua, P. C., Kierzek, R., Johnson, K. A., and Turner, D. H. (1992) *Science 258*, 1355−1358.
4. Herschlag, D., Eckstein, F., and Cech, T. (1993) *Biochemistry 32*, 8312−8321.
5. Strobel, S. A., and Cech, T. R. (1993) *Biochemistry 32*, 13593−13604.
6. Strobel, S. A., and Cech, T. R. (1995) *Science 267*, 675−679.
7. Herschlag, D. (1992) *Biochemistry 31*, 1386−1399.
8. Strobel, S. A., and Cech, T. R. (1994) *Nat. Struct. Biol. 1*, 13−17.
9. Altman, S., Kirsebom, L., and Talbot, S. (1993) *FASEB J. 7*, 7−14.
10. Pace, N. R., and Brown, J. W. (1995) *J. Bacteriol. 177*, 1919−1928.
11. Guerrier-Takada, C., Gardiner, K., Marsh, T., Pace, N., and Altman, S. (1983) *Cell 35*, 849−857.
12. Beebe, J. A., and Fierke, C. A. (1994) *Biochemistry 33*, 10294−10304.

13. McClain, W. H., Guerrier-Takada, C., and Altman, S. (1987) *Science 238*, 527−530.
14. Kahle, D., Wehmeyer, U., and Krupp, G. (1990) *EMBO J. 9*, 1929−1937.
15. Thurlow, D. L., Shilowski, D., and Marsh, T. L. (1991) *Nucleic Acids Res. 19*, 885−891.
16. Kirsebom, L. A., and Svard, S. G. (1994) *EMBO J. 13*, 4870−4876.
17. LaGrandeur, T. E., Huttenhofer, A., Noller, H. F., and Pace, N. R. (1994) *EMBO J. 13*, 3945−3952.
18. Loria, A., and Pan, T. (1997) *Biochemistry 36*, 6317−6325.
19. Westhof, E., and Altman, S. (1994) *Proc. Natl. Acad. Sci. U.S.A. 91*, 5133−5137.
20. Harris, M. E., Nolan, J. M., Malhotra, A., Brown, J. W., Harvey, S. C., and Pace, N. R. (1994) *EMBO J. 13*, 3953−3963.
21. Scaringe, S. (1996) Ph.D. Thesis, University of Colorado at Boulder, Boulder, CO.
22. Pan, T. (1995) *Biochemistry 34*, 902−909.
23. Fersht, A. (1985) in *Enzyme structure and mechanism*, 2nd ed., pp 109−111, 137−138, W. H. Freeman and Co., New York.
24. Smith, D., and Pace, N. R. (1993) *Biochemistry 32*, 5273−5281.
25. Pan, T., Loria, A., and Zhong, K. (1995) *Proc. Natl. Acad. Sci. U.S.A. 92*, 12510−12514.
26. Oh, B.-K., and Pace, N. R. (1994) *Nucleic Acids Res. 22*, 4087−4094.
27. Krupp, G., Kahle, D., and Vogt, T. (1991) *J. Mol. Biol. 217*, 637−648.
28. Holm, P. S., and Krupp, G. (1992) *Nucleic Acids Res. 20*, 421−423.
29. Svard, S. G., and Kirsebom, L. A. (1992) *J. Mol. Biol. 227*, 1019−1031.
30. Kufel, J., and Kirsebom, L. A. (1996) *J. Mol. Biol. 263*, 685−698.
31. Kufel, J., and Kirsebom, L. A. (1996) *Proc. Natl. Acad. Sci. U.S.A. 93*, 6085−6090.
32. Guerrier-Takada, C., Lumelsky, N., and Altman, S. (1989) *Science 246*, 1578−1584.
33. Wawrousek, E. F., Narasimhan, N., and Hansen, J. N. (1984) *J. Biol. Chem. 259*, 3694−3702.
34. Green, C. J., Stewart, G. C., Hollis, M. A., Vold, B. S., and Bott, K. F. (1985) *Gene 37*, 261−266.
35. Garrity, D., and Zahler, S. (1993) *J. Bacteriol. 175*, 6512−6517.
36. Kurz, J. C., Niranjanakumari, S., and Fierke, C. A. (1998) *Biochemistry 37*, 2393−2400.
37. Kirsebom, L. A., and Svard, S. G. (1992) *Nucleic Acids Res. 20*, 425−432.
38. Steitz, T. A., and Steitz, J. A. (1993) *Proc. Natl. Acad. Sci. U.S.A. 90*, 6498−6502.
39. Warnecke, J. M., Furste, J. P., Hardt, W.-D., Erdmann, V. A., and Hartmann, R. K. (1996) *Proc. Natl. Acad. Sci. U.S.A. 93*, 8924−8928.

BI980220D